[18F]-FDG PET and MRI radiomic signatures to predict the risk and the location of tumor recurrence after re-irradiation in head and neck cancer

Arnaud Beddok, Fanny Orlhac, Valentin Calugaru, Laurence Champion, Catherine Ala Eddine, Christophe Nioche, Gilles Créhange, Irène Buvat

[18F]-FDG PET and MRI radiomic signatures to predict the risk and the location of tumor recurrence after re-irradiation in head and neck cancer

Short title: *radiomics in head and neck cancer reirradiation*

Arnaud Beddok[1,2], Fanny Orlhac[1], Valentin Calugaru[2], Laurence Champion[1,3], Catherine Ala Eddine[4], Christophe Nioche[1], Gilles Crehange[2], Irène Buvat[1]

1. Institut Curie, PSL Research University, University Paris Saclay, Inserm LITO U1288 Orsay, France
2. Institut Curie, PSL Research University, Radiation Oncology Department, Paris/Orsay, France.
3. Institut Curie. Department of Nuclear Medicine. Saint-Cloud. France.
4. Institut Curie. Department of Radiology. Paris. France

Corresponding author: Arnaud Beddok, Department of Radiation Oncology, 25 rue d'Ulm 75005 Paris; +33169298721; arnaud.beddok@curie.fr; a.beddok@gmail.com; ORCID: 0000-0002-5512-4161

Number of words: 5800/6000 (including references)

Number of tables/pictures: 6/6

ABSTRACT

Purpose: To evaluate whether radiomics from [18F]-FDG PET and/or MRI before re-irradiation (reRT) of recurrent head and neck cancer (HNC) could predict the occurrence and the location “in-field” or “outside” of a second locoregional recurrence (LR).

Methods: Among the 55 patients re-irradiated at curative intend for HNC from 2012 to 2019, 48 had an MRI and/or PET before the start of the reRT. Thirty-nine radiomic features (RF) were extracted from the reirradiated GTV (rGTV) using LIFEx software. Student t-tests and Spearman Correlation Coefficient were used to select the RF that best separate patients who recurred from those who did not, and “in-field” from “outside” recurrences. Principal component analysis involving these features only was used to create a prediction model. Leave-one-out cross-validation was performed to evaluate the models.

Results: After a median follow-up of 17 months, 40/55 patients had developed a second LR, including 18 “in-field” and 22 “outside” recurrences. From pre-reRT MRI, a model based on three RF (GLSZM_SZHGLE, GLSZM_LGLZE and skewness) predicted whether patients would recur with a balanced accuracy (BA) of 83.5%. Another model from pre-reRT MRI based on three other RF (GLSZM_ LZHGE, NGLDM_Busyness and GLZLM_SZE) predicted whether patients would recur “in-field” or “outside” with a BA of 78.5%. From pre-reRT PET, a model based on four RF (Kurtosis, SUVbwmin, GLCM_Correlation and GLCM_Contrast) predicted the LR location with a BA of 84.5%.

Conclusion: RF characterizing tumor heterogeneity extracted from pre-reRT PET and MRI predicted whether patients would recur, and whether they would recur "in-field" or "outside".

Keywords: re-irradiation; head and neck cancer; radiomics; multimodal imaging.

1. INTRODUCTION

Despite the numerous innovations in radiation therapy (RT) in the last few years, in particular the development of intensity-modulated radiation therapy (IMRT) and the use of new targeted therapies in combination with RT [1], the risk of local recurrence after a first irradiation for head and neck cancer (HNC), particularly in the skull base, remains high [2,3]. The therapeutic modality most frequently used for the management of these local recurrences is surgery whenever possible [4–6]. Nevertheless, in some cases, surgery is not possible, either because the tumor infiltrates adjacent structures, especially vessels, and becomes unresectable, or because the patient is not operable due to comorbidities. In this case, the indication of a re-irradiation (reRT), with or without chemotherapy, is increasingly discussed in multidisciplinary staff. However, the risk of a second recurrence after reRT remains also very high. In a recent meta-analysis that reported the outcomes of 1635 patients reirradiated for recurrent HNC, more than half of the patients developed a second recurrence within two years of the end of the reRT [7]. Furthermore, in a recent pattern-of-failure study, Margalit *et al* reported that approximately half of these second local recurrences occurred within the re-irradiated GTV (rGTV), while the other half occurred outside the field (34%) or at the margin (14%) of the isodose line of prescription [8].

The selection of patients for reRT is complex, especially considering the high risk of severe toxicities occurring within the two years following radiotherapy (up to 50%) [9]. Thus, a prediction of the risk of a second recurrence would allow the selection of patients for whom this treatment modality is the best option or to consider an alternative treatment. Several nomograms have been proposed to help the radiation oncologist for this patients selection but have not been widely adopted [10–13]. Moreover, none of these nomograms has included radiomic analysis of pre-reRT images. In addition, prior knowledge of whether the recurrence is likely to occur in field or outside could enable adapting the treatment of these patients. For patients at high risk of in-field recurrence, the dose could be escalated in the areas at highest risk of recurrence [14,15]. For patients at high risk of recurrence outside the GTV, their surveillance could be adapted. In addition, predicting the location of this second recurrence would be useful to define the target volume, as there is currently no consensus on the CTV margins to be applied around the rGTV [16].

Several recent studies have shown that multimodal imaging, especially PET and MRI, and radiomics, could be useful to predict the risk of recurrence and to discriminate the regions with the highest and lowest risks of recurrence. In a recent study, Zhao et al. identified in a large cohort of recurrent nasopharyngeal carcinomas deep learning signatures from pre-reRT PET associated with overall survival [17]. Furthermore, in a small series of fourteen patients irradiated for nasopharyngeal carcinoma, Akram *et al.* have shown that several radiomic features extracted from pre-treatment MRI were significantly different between recurrent and non-recurrent regions [18]. Moreover, Yan *et al.* showed in a study including 28 patients that the maximum standardized uptake value (SUVmax) and a dose response matrix from multiple FDG-PET/CT images obtained before and during the first weeks of chemotherapy for head and neck squamous cell carcinomas could predict local recurrence [19].

The objective of our study was to determine whether multimodal imaging, including [18F]-FDG PET and MRI, together with radiomics, could be useful to predict the risk of second recurrence of HNC and the “in-field” or

"outside" location of this second recurrence, with the objective of selecting recurrent HNC patients that would most benefit from reRT and to optimize treatment plans in this setting.

2. MATERIAL AND METHODS

2.1. Patients

From August, 2012 to April, 2019, 55 patients received reRT at Institut Curie for a recurrent HNC. The diagnosis of local relapse after the initial RT was proven by biopsy or surgical specimen. The reRT was delivered after surgery when complete resection was not obtained or without surgery when lesions appeared to be unresectable. The treatment of each patient was discussed by a multidisciplinary team. After the end of the reRT, MRI, CT, and/or PET/CT scans of the neck were performed every six months during the first five years, and every 12 months thereafter or until death. Locoregional failure (LRF) was detected within the head and neck by either clinical examination, and/or imaging, and/or biopsy. This study was approved by the Ethics Committee of Institut Curie on 07/07/20. Re-irradiation parameters were reported in a previous study[20].

2.2. Image acquisition

All patients included in this study had [18F]-FDG PET and/or MRI before the reRT and at the time of local recurrence. Several different devices were used for [18F]-FDG PET imaging: DISCOVERY STE, DISCOVERY IQ, DISCOVERY MI, DISCOVERY 610 ELITE, DISCOVERY 710, DISCOVERY 690 from GE Healthcare and GEMINI, GEMINI GXL from Philips. Median blood glucose level was 5.2 mmol/l (IQR: 5.1 – 6.1). Median time after FDG injection was 60 min (IQR: 60 – 63.8). [18F]-FDG PET characteristics are summarized in **Sup. Table 1**. MRI were acquired on Siemens Symphony Tim, Siemens Aera, Siemens AVANTO FIT, GE Optima MR450 scanners. Gadopentetate dimeglumine at 0.1 mmol/kg of body weight was administered for contrast enhanced scans. Out of the various MRI sequences that were acquired for each patient, we selected the contrast-enhanced fat-suppressed T1-weighted spin echo sequence for analysis [21]. The median voxel size was 0.74 mm^3 (IQR: 0.45 – 1.01). The N4 parametric bias field correction (Slicer software [22]) was used for correcting the nonuniform intensity in MRI [23].

2.3. Image analysis

The pre-reRT [18F]-FDG PET and/or MRI were fused with CT simulation images using rigid registration with Eclipse treatment planning system (Varian Medical Systems, Palo Alto, California). All reirradiated GTV (rGTV) were delineated at the time of recurrence diagnosis. Using the PET images, the rGTV was segmented based on the hypermetabolism defined as SUV > 3. Using the MRI images, the rGTV was segmented based on the contrast enhancement. These fused pre-treatment MRI and/or PET and CT images together with the rGTV contours and 95% isodose lines were retrieved from Eclipse Treatment Planning System.

Thirty-nine radiomic features were extracted from rGTV using LIFEx software v 7.0.10 [24] after 2x2x2mm^3 spatial resampling and a fixed bin size of 0.157 SUV units between 0 and 20 SUV for PET images, and 1x1x1mm^3 spatial resampling and a relative intensity rescaling with 128 grey levels between the minimum and maximum value in the rGTV for MRI. In the PET images, these 39 radiomic features included three SUVs (SUVmin, SUVmax and SUVpeak), five first order statistics derived from the gray-level histogram: mean, variance, skewness, kurtosis,

excess kurtosis and 31 textural features. **Sup.Figure 1** summarized the radiomics workflow for [18F]-FDG PET imaging analysis. In the MRI images, the same features were calculated, except that the three SUVs were replaced by three MR intensity values: minimum intensity in the rGTV, maximum intensity in the rGTV, and mean intensity in the 1 mL sphere that contained the largest mean value in the rGTV. **Sup. Table 2** summarized the 31 extracted textural features.

2.4. Pattern of failure study

For all patients with locoregional relapse or second primary HNC after reRT, the recurrent tumor volume (Vrecur) was identified in the MRI and/or PET images obtained at the time of diagnosis of second recurrence. The contours of this volume were validated for each patient by at least a nuclear physician (LC) and/or a radiologist (CAE) expert in this pathology. The exact site and extent of each recurrent tumor were then compared to the pretreatment planning CT datasets, focusing on the 95% isodose lines. The recurrences were categorized according to previously published criteria [25] as occurring inside or outside the irradiated targets: the Vrecur was deemed "in-field" if the majority of Vrecur was within the 95% isodose; "marginal" if > 20 % and ≤ 50% of Vrecur was within the 95% isodose; or "outside" if less than 20% of the Vrecur was inside the 95% isodose (**Figure 1**).

2.5. Statistical analysis

Follow-up duration was calculated from the date of the end of reRT to the last clinical follow-up. Baseline characteristics were summarized as numbers and percentages for qualitative data, and as means and standard deviations or medians with the minimum and maximum (or inter-quartile range) for continuous variables. Overall survival (OS) was defined as the time between the date of the end of reRT and the date of death for deceased patients. Patients still alive were censored at the date of their last news. Locoregional failure-free survival (LFFS), including local and nodal progression, was calculated from the date of the end of reRT until the date of LRF. In the absence of any event, patients were censored at the date of their last news. Survival distributions were estimated by the Kaplan – Meier method.

This radiomics analysis was divided in two parts. A first study aimed at separating patients who developed recurrence from patients who did not relapse based on the PET and/or MR radiomic features measured before reRT. A second study investigated whether we could distinguish between patients who developed recurrence in-field from patients whose recurrence was outside the rGTV based on the PET and/or MR radiomic features measured before reRT. For both studies, Shapiro-Wilk normality tests were carried out on the differences observed between the groups (group recurrence vs. group no recurrence on one hand, group in-field vs. group outside on the other hand) for the 39 features, and p-values < 0.05 were considered significantly different. Paired t-tests were performed on the features and Wilcoxon signed-rank tests were carried out on the features that violated the normality assumption. Spearman Correlation Coefficient values with p-values and correlograms were computed for the features that were significantly different between groups, to identify features reflecting similar information. Principal component analysis (PCA) was then performed on features that were significantly different between the groups to reduce dimensionality and determine whether patients from the two groups could be linearly separated in that space. Wilks's test was applied to test whether the barycenter of the two groups had

significantly different coordinates in the two-dimensional (2D) space built using the first two principal components, a $p < 0.05$ indicating that the barycenter had significantly different coordinates.

Given the small number of patients, leave-one-out cross-validation was performed to validate the prediction model established from the PCA projections. In brief, PCA space generated by the first 2 principal components was created on N-1 patients. Based on the analysis of the data in this 2D space, an optimal cut-off was determined on the first dimension only (the second dimension had no separating power) to maximize the Youden index (sensitivity + specificity -1) for separating the 2 groups. Then, the N^{th} patient was projected in the PCA space and was assigned to one of the 2 groups as a function of its position with respect to the cut-off. This assignment was compared to the true patient classification. The process was repeated for all the N patients. A confusion matrix was then constructed to determine the performance of the model. Balanced accuracy (optimal value = 100%), Sensitivity (optimal value = 100%), and Specificity (optimal value = 100%) were reported to assess the performance of the prediction model. A permutation test was then performed (100 repetitions) for each situation in order to assess the significance of the results.

In addition, for each classification task, Receiver Operator Characteristic (ROC) analysis were performed on the whole cohorts (without any leave-one-out strategy) to compute Area Under the Curve (AUC) and 95% CI were estimated by 2000 boostraps [26]. Similarly, using the whole cohort, Harrell's concordance index (C-index) was used to assess the performance of the prediction model using pre-reRT MRI to predict the recurrence time.

All statistical analyses were performed using R software [27].

3. RESULTS

3.1. Population

The basal characteristics of these 55 patients are summarized in **Table 1.** The majority of patients were males (70.9%) and the median age was 51 (IQR: 47.5 – 61). The main sites of recurrence were the nasopharynx (N=13), the nasal cavity and paranasal sinus (N=11), the oropharynx (N=8), and the regional lymph nodes (upper jugular group, retropharyngeal, retrostyloid, N=7). Half of these patients were re-irradiated with proton while the other half were re-irradiated using X-rays (mainly intensity-modulated radiation therapy [IMRT]). The median follow-up for the entire cohort was 17 months (IQR: 7 – 41), and the median OS was 32 months (IQR: 17 – 46). The one- and two-years OS were 71% [95% CI: 60%-84.7%] and 56% [43%-72%], respectively (**Figure 2A**). Over the follow-up period, 40/55 (72%) patients have developed a second locoregional recurrence, including 18 "in-field" and 22 "outside" recurrences. None of the recurrences was "marginal". Histological verification of second recurrent tumor was available in 18/40 cases. The one- and two-years LFFS were 53% [95% CI: 41%-69%] and 29% [18%-45%], respectively (**Figure 2B**). The OS and the LFFS were not significantly different between the "on-field" and "outside" groups ($p = 0.56$, Sup Figure 2A and $p=0.43$, Sup Figure 2B, respectively).

Among the 55 included patients, 87.3% had pre-re-irradiation imaging and could be included in the radiomic analysis (**Figure 3**). Among the 33 patients with MR imaging before reRT, 21 developed a second locoregional recurrence, including 9"in-field" and 12 "outside" recurrences. Among the 30 patients with PET imaging before

reRT, 23 developed locoregional recurrences, including 9 “in-field” and 14 “outside” recurrences. There was no “marginal” recurrence. Among the 40 patients with locoregional recurrences, 10 had PET and MRI before the reRT.

3.2. Prediction of the recurrence

Among the 39 extracted features from the reirradiated GTV segmented on MRI, eight were significantly different ($p < 0.05$) between the patients who developed recurrences and the patients who did not: Skewness from the gray-level histogram, three features calculated from the Gray-Level Run Length Matrix (GLRLM): High Grey Level Run Emphasis (HGLRE), Short Run High Grey Level Emphasis (SRHGLE), and Long Run High Grey Level Emphasis (LRHGLE), and 4 features calculated from the Gray Level Size Zone Matrix (GLSZM): Low Gray Level Zone Emphasis (LGLZE), High Gray Level Zone Emphasis (HGLZE), Small Zone Low Grey Level Emphasis (SZLGLE), and Small Zone High Grey Level Emphasis (SZHGLE) (**Sup Figure 3**).

The correlation analysis between these eight features (**Sup. Fig. 4)** showed that many of the eight selected features had a strong correlation (Spearman correlation coefficient $r_s > 0.8$). For further analysis, we selected only the three features that were the least correlated with the others ($r_s \leq 0.8$): SZHGLE, LGLZE and skewness. Each pre-RT GTV was thus characterized by these three feature values. To further reduce dimensionality, a principal component analysis (PCA) was applied on the set of 33 vectors of three features (one vector per patient that had an MRI before reRT). The first two dimensions of the space spanned by the principal components (PC) expressed 88.5% of the total dataset variance. The group of patients with recurrence was well separated from the group of patients without recurrence in that 2D-space ($p < 0.02$) (**Figure 4**). “Recurrence” group corresponded to regions with high SZHGLE and low LGLZE and skewness (**Sup. Figure 5**). Leave-one-out cross-validation confirmed the excellent balanced accuracy of the model = 84% (Se = 91%, Spe = 76%) with only six patients misclassified (one “recurrence” classified as “no recurrence” and five “no recurrences” classified as “recurrences”). These results were significantly higher than those from the permutation experiment ($p<0.05$, **Sup. Figure 6**). The AUC from ROC analysis was 0.85 [95%CI: 0.72-0.98]. The Harrell’s C-Index of this pre-reRT MRI radiomic signature was 64%.

Among the 39 features extracted from the reirradiated GTV segmented on PET, only the Coarseness textural feature calculated from the Neighborhood Gray-Level Different Matrix (NGLDM) was significantly lower ($p < 0.05$) for the patients who developed recurrences compared to the patients who did not (**Sup. Figure 7**). Based on this feature, the leave one out cross validation found a balanced accuracy = 69% (Se = 42%, Spe = 95%) with five out of 30 patients misclassified (one “recurrence” classified as “no recurrence” and four “no recurrences” classified as “recurrences”). This result was not significantly higher than the one obtained with the permutation experiment ($p = 0.09$, **Sup. Figure 8**). The AUC from ROC analysis was 0.64 [95% CI: 0.30-0.97].

3.3. Prediction of the location of the recurrence from MRI

Among the 39 features extracted from the reirradiated GTV segmented on MRI, ten were significantly different ($p < 0.05$) between the patients who had “in-field” and “outside” recurrences: Contrast from the Gray Level Co-occurrence Matrix (GLCM), 3 from the GLRLM: Short Run Emphasis (SRE), Long Run Emphasis (LRE) and Run

Percentage (RP), 3 from the NGLDM: Contrast, Busyness and Coarseness, 3 from GLSZM: Small Zone Emphasis (SZE), Large Zone High Gray Emphasis (LZHGE), and Zone Percentage (ZP) (**Sup. Figure 9**).

The correlation analysis between the features showed that most of these 10 selected features were strongly correlated ($r_s > 0.8$). For subsequent analysis, we selected only the three features that were the least correlated with the others ($r_s \leq 0.8$): LZHGE, Busyness, and SZE (**Sup. Figure 10**). Principal component analysis (PCA) was applied on the set of 21 vectors (corresponding to the 21 patients with MR who experienced recurrence) of these three significant features. The first two dimensions of the PCA space expressed 89.5% of the variance. In that 2-dimensional PCA space, the "in-field" and "outside" groups were well separated ($p < 0.02$) (**Figure 5A**). "In-field" group corresponded to regions with high LZHGE and Busyness, whereas "Outside" group corresponded to regions with high SZE (**Sup. Figure 11**). Leave-one-out cross-validation yielded a 79% balanced accuracy of the model (Se = 66%, Spe = 91%with only four patients out of 21 misclassified (three "in-field" classified as "outside" and one "outside" classified as "in-field"). These results were significantly higher than those from the permutation experiment ($p<0.05$, **Sup. Figure 12**). All the ten patients with MRI and PET before reRT were well classified with this MRI based predictive model. The AUC from ROC analysis was 0.85 [95% CI: 0.66-1].

3.4. Prediction of the location of the recurrence from PET

Among the 39 features extracted from the reirradiated GTV segmented on PET, four were significantly different ($p < 0.05$) between the patients who had "in-field" and "outside" recurrences: Kurtosis, SUVmin, and Correlation and Contrast from the GLCM (**Sup. Figure 13**).

The correlation analysis showed that these four features were not strongly correlated ($r_s \leq 0.8$) (**Sup. Figure 14**). All four were then used for further PCA analysis. The first two dimensions of PCA expressed 75.1% of the total variance. Again, the "in-field" and "outside" rGTV groups were well separated in a 2D-space spanned by these first two principal components ($p < 0.02$) (**Figure 5B**). "In-field" group corresponded to regions with high GLCM_Contrast and GLCM_Correlation, and low Kurtosis and SUV min (**Sup. Figure 15**). Leave-one-out cross-validation yielded a 84.5% balanced accuracy of the model (Se = 77%, Spe = 92%) with only three patients misclassified out of 23 (two "in-field" classified as "outside" and one "outside" classified as "in-field"). These results were significantly higher than those obtained using the permutation experiment ($p < 0.05$, **Sup. Figure 16**). The AUC from ROC analysis was 0.84 [95%CI: 0.63-1]. Among the ten patients with PET and MRI before reRT, nine were well classified with this PET based predictive model.

4. DISCUSSION

In the present study, we have reported the outcomes of 55 patients with recurrent HNC reirradiated for curative intend with X-rays (essentially VMAT) or protontherapy (PSPT). The two-year OS observed in the present study (55.6% [43.2%-71.7%]) was consistent with the two-year OS reported in two recent meta-analyses that analyzed the outcomes of patients reirradiated with IMRT for recurrent HNC: 45.7% (95% CI: 41.4%-50.1%) (17 trials) [7] and 41.3% (95% CI: 37.3%–45.7%) (39 studies included 3766 patients) [28], respectively. The two-year LFFS observed in our study was 28.6% [18.1%-45.1%]. This is relatively low compared to the two-year LFFS reported in

both sub-mentioned meta-analyses: 51.9% (95% CI: [46.4%-57.3%]) and 48.8% (95% CI: [43.7%–54.5%]), respectively. Yet, in Dionisi's meta-analysis, the included series were highly heterogeneous (I^2=82.7%, P < 0.0001), with different location, histology, combination of treatment (surgery, chemotherapy). However, the two-year LFFS observed in our series was similar to the two-year LFFS in Popovtzer et al.'s study [29], in which the authors included a majority of skull base tumors. Besides, the relatively low LFFS observed in our study could be due to the size of the target volumes, with a median reRT CTV and PTV of 49.2 mL and 104.4 mL, respectively. Indeed, in a prospective study including 21 patients reirradiated for a recurrence of HNC, Chen *et al.* showed that the only identified parameter predictive of local recurrence was the planning target volume [30]. Patients with a tumor volume > 27 mL had a worse prognosis. Among the 40 patients with second locoregional recurrence, we observed 18 (45%) "in-field" and 22 (55%) "outside" recurrences. This is consistent with the results reported by Margalit *et al.* [8] who reported 48.6% "in-field" and 48.5% "outside" or "marginal" locoregional recurrences (2.9% unknown). In contrast to Margalit et al, we did not find any association between surgery vs. no surgery status and "in-field" or "outside" location of recurrence.

In our study, we have attempted to provide as much information as possible to ensure that our data can be easily replicated by other teams to validate our findings. Indeed, rapid advances in automated methods for extracting large numbers of quantitative features from medical images have led to an explosion of publications exploring combinations of features as potential imaging biomarkers for diagnosis, clinical prognosis, treatment selection, or other decision support [31]. However, to the best of our knowledge, sophisticated radiomic signatures identified through a high-throughput pipeline are not used in the clinic [32]. One reason is the lack of independent external validation studies that could confirm the performance of the models and demonstrate their generalizability to different groups of patients. This lack of external validation is partly due to insufficient information provided in publications to allow replication of the models in external validation cohorts [33]. In 2020, Norgeot *et al.* provided a check list of the minimal information that should be completed in a radiomic original research to allow rapid replication and validation of radiomic and artificial intelligence based models [34]. The completed checklist can be found in Sup. Table 3, to encourage other teams to replicate our study and test our models.

To the best of our knowledge, the present work is the first study assessing the predictive value of PET and MR radiomics features in the field of reirradiation for HNC. We found that before reRT, MRI radiomics features characterizing local grey-level intensity in the GTV to be re-irradiated had different values in patients who will relapse "in-field" or "outside": "in-field" recurrences were associated with locally less uniform texture in the GTV, whereas "outside" relapses were associated with locally more uniform texture in the GTV. Several previously published studies have also reported the predictive value of intratumoral heterogeneity for patients irradiated for the first time for HNC. In a study involving pre-irradiation MRI, Alfieri *et al.* found a signature associated with the patients outcomes that included three radiomics features correlated with tumor heterogeneity [35]. Akram et al. also performed a radiomics study in 14 patients irradiated with IMRT for nasopharyngeal carcinoma. A total of seven radiomics features extracted from pre-irradiation MRI and reflecting heterogeneity were significantly different between the recurrent and the non-recurrent regions [18].

We also found that before reRT, [18F]-FDG PET radiomics features characterizing the signal heterogeneity in the GTV to be re-irradiated had different values in patients who will relapse “in-field” or “outside”, further supporting the presence of biological information associated with the tumor aggressiveness captured by the images: “in-field” relapses were associated with higher metabolic heterogeneity in the GTV and “outside” relapses were associated with higher metabolic homogeneity in the GTV. In 2017, Bogowicz et al. have investigated the prognostic value of different radiomics features extracted from post-irradiation [18F]-PET of patients with HNC [36]. The prognostic model for local tumor control showed a good discriminative power with a concordance index higher than 0.7 in their both training and validation cohorts. This study showed that the heterogeneity of [18F]-FDG activity in the region of primary tumor observed 3 months post-irradiation was related to the risk of tumor recurrence. Higher histogram range and higher GLCM difference entropy corresponded to higher risk of tumor recurrence. This study therefore supports the idea that radiomic parameters related to tumor contrast could carry information on the risk of local recurrence. In a recent study, Zhao *et al.* studied the predictive value of pre-reRT PET to identify patients with high or low prognostic after reRT for recurrent nasopharyngeal carcinoma [17]. They showed that PET/CT-based deep learning signatures were associated with overall survival and could be included in a nomogram to guide individual treatment. We could not replicate the model proposed in this study because some information was missing, in particular the precise definition of the region of interest, the extraction method of the studied image parameters and the selection of the studied features. In addition, this study involved only recurrent nasopharyngeal cancers and the authors did not explicit the deep learning signatures, making it impossible to reproduce their nomogram.

It should also be noted that among the ten patients with locoregional recurrences who had PET and MRI before reRT, nine were well classified with the two modalities based predictive models. Thus when the two modalities yielded the same classification, it was always correct. One patient was well classified on MRI but misclassified on PET. The combination of both modalities might thus be a relevant approach to increase the confidence in the classification. This is consistent with several recent studies that have shown that PET/MRI devices allow to precisely determine the pattern of failure of local recurrence of head and neck cancer after a first irradiation [37,38] and help the radiation oncologist in the staging and later treatment response evaluation in HNC [39].

The main limitations of our series are that it was retrospective, single-center and included a small number of patients, although our series in the largest of its kind published in the literature so far. This small number of patients is explained by the rigorous selection procedure: all included patients had to have been treated for an HNC with curative intent, and to have a minimum follow-up of 4 months. All patients included in the radiomic analysis were also required to have undergone PET and/or MRI imaging prior to reRT. Another limitation is the heterogeneity of the included patients with in particular different pathologies and different re-irradiation techniques (including a large portion of patients receiving protons). Preliminary studies were first performed by including only patients reirradiated with protons. Once the model was created, the data of patients reirradiated with photons were projected in the PCA plan. Sup. Figures 17-19 show that the majority of patients reirradiated with photons were well classified, for the status “recurrence” vs “no recurrence” and the pattern “in-field” and “outside”. The same type of analysis was performed by including only patients reirradiated for squamous cell

carcinoma. Once the model was created, the data of patients reirradiated for other pathology subtypes were projected in the PCA plan. **Sup. Figures 20 and 21** show that the majority of patients reirradiated for other pathology subtypes were well classified, both for the status “recurrence” vs “no recurrence” and the pattern “in-field” and “outside”.

In conclusion, the present study showed that radiomic features extracted from pre-reirradiation PET and MRI scans and reflecting intratumoral heterogeneity could predict the risk and the location of second recurrence for patients with recurrent head and neck cancer. All data were provided to allow rapid external validation based on a prospective cohort of a larger number of patients.

5. FUNDING

The authors declare that no funds, grants, or other support were received during the preparation of this manuscript.

6. DECLARATIONS

Conflict of Interest: The authors have no relevant financial or non-financial interests to disclose.

Consent to participate: The ethical review board of Institut Curie approved this retrospective study and waived the requirement of informed consent.

Data availability statement: The data that support the findings of this study are available from the corresponding author upon reasonable request.

Ethics approval: All procedures performed in the study and involving human participants were carried out in accordance with the ethical standards of the institutional and/or national research committee and with the principles of the 1964 Declaration of Helsinki and its later amendments or comparable ethical standards.

Authors’ contribution: Conception and design: A. Beddok and I. Buvat; Collection and assembly of data: A. Beddok; Data analysis and interpretation: A. Beddok, F. Orlhac and I. Buvat; Manuscript writing: A. Beddok and I. Buvat; Final approval of manuscript: Arnaud Beddok, Fanny Orlhac, Valentin Calugaru, Laurence Champion, Catherine Ala Eddine, Christophe Nioche, Gilles Crehange, and Irène Buvat.

7. REFERENCES

1. Tao Y, Aupérin A, Sun X, Sire C, Martin L, Coutte A, et al. Avelumab-cetuximab-radiotherapy versus standards of care in locally advanced squamous-cell carcinoma of the head and neck: The safety phase of a randomised phase III trial GORTEC 2017-01 (REACH). Eur J Cancer. 2020;141:21–9.

2. Cooper JS, Zhang Q, Pajak TF, Forastiere AA, Jacobs J, Saxman SB, et al. Long-term follow-up of the RTOG 9501/intergroup phase III trial: postoperative concurrent radiation therapy and chemotherapy in high-risk squamous cell carcinoma of the head and neck. Int J Radiat Oncol Biol Phys. 2012;84:1198–205.

3. Setton J, Caria N, Romanyshyn J, Koutcher L, Wolden SL, Zelefsky MJ, et al. Intensity-Modulated Radiotherapy in the Treatment of Oropharyngeal Cancer: An Update of the Memorial Sloan-Kettering Cancer Center Experience. International Journal of Radiation Oncology*Biology*Physics. 2012;82:291–8.

4. Nichols AC, Kneuertz PJ, Deschler DG, Lin DT, Emerick KS, Clark JR, et al. Surgical salvage of the oropharynx after failure of organ-sparing therapy. Head & Neck. 2011;33:516–24.

5. Bachar GY, Goh C, Goldstein DP, O'Sullivan B, Irish JC. Long-term outcome analysis after surgical salvage for recurrent tonsil carcinoma following radical radiotherapy. Eur Arch Otorhinolaryngol. 2009;267:295.

6. Taussky D, Dulguerov P, Allal AS. Salvage surgery after radical accelerated radiotherapy with concomitant boost technique for head and neck carcinomas. Head & Neck. 2005;27:182–6.

7. Lee J, Shin I-S, Kim WC, Yoon WS, Koom WS, Rim CH. Reirradiation with intensity-modulated radiation therapy for recurrent or secondary head and neck cancer: Meta-analysis and systematic review. Head Neck. 2020;42:2473–85.

8. Margalit DN, Rawal B, Catalano PJ, Haddad RI, Goguen LA, Annino DJ, et al. Patterns of failure after reirradiation with intensity-modulated radiation therapy and the competing risk of out-of-field recurrences. Oral Oncology. 2016;61:19–26.

9. Margalit DN, Schoenfeld JD, Rawal B, Haddad RI, Catalano PJ, Goguen LA, et al. Patient-oriented toxicity endpoints after head and neck reirradiation with intensity modulated radiation therapy. Oral Oncol. 2017;73:160–5.

10. Tanvetyanon T, Padhya T, McCaffrey J, Zhu W, Boulware D, Deconti R, et al. Prognostic factors for survival after salvage reirradiation of head and neck cancer. J Clin Oncol. 2009;27:1983–91.

11. Ward MC, Riaz N, Caudell JJ, Dunlap NE, Isrow D, Zakem SJ, et al. Refining Patient Selection for Reirradiation of Head and Neck Squamous Carcinoma in the IMRT Era: A Multi-institution Cohort Study by the MIRI Collaborative. International Journal of Radiation Oncology*Biology*Physics. 2018;100:586–94.

12. Ward MC, Lee NY, Caudell JJ, Zajichek A, Awan MJ, Koyfman SA, et al. A competing risk nomogram to predict severe late toxicity after modern re-irradiation for squamous carcinoma of the head and neck. Oral Oncol. 2019;90:80–6.

13. Riaz N, Hong JC, Sherman EJ, Morris L, Fury M, Ganly I, et al. A nomogram to predict loco-regional control after re-irradiation for head and neck cancer. Radiother Oncol. 2014;111:382–7.

14. Skjøtskift T, Evensen ME, Furre T, Moan JM, Amdal CD, Bogsrud TV, et al. Dose painting for re-irradiation of head and neck cancer. Acta Oncol. 2018;57:1693–9.

15. Welz S, Paulsen F, Pfannenberg C, Reimold M, Reischl G, Nikolaou K, et al. Dose escalation to hypoxic subvolumes in head and neck cancer: A randomized phase II study using dynamic [18F]FMISO PET/CT. Radiother Oncol. 2022;171:30–6.

16. Ward MC, Koyfman SA, Bakst RL, Margalit DN, Beadle BM, Beitler JJ, et al. Retreatment of Recurrent or Second Primary Head and Neck Cancer After Prior Radiation: Executive Summary of the American Radium Society® (ARS) Appropriate Use Criteria (AUC): Expert Panel on Radiation Oncology - Head and Neck Cancer. Int J Radiat Oncol Biol Phys. 2022;S0360-3016(22)00280-2.

17. Zhao X, Liang Y-J, Zhang X, Wen D-X, Fan W, Tang L-Q, et al. Deep learning signatures reveal multiscale intratumor heterogeneity associated with biological functions and survival in recurrent nasopharyngeal carcinoma. Eur J Nucl Med Mol Imaging. 2022;49:2972–82.

18. Akram F, Koh PE, Wang F, Zhou S, Tan SH, Paknezhad M, et al. Exploring MRI based radiomics analysis of intratumoral spatial heterogeneity in locally advanced nasopharyngeal carcinoma treated with intensity modulated radiotherapy. Woloschak GE, editor. PLoS ONE. 2020;15:e0240043.

19. Yan D, Chen S, Krauss DJ, Chen PY, Chinnaiyan P, Wilson GD. Tumor Voxel Dose-Response Matrix and Dose Prescription Function Derived Using 18F-FDG PET/CT Images for Adaptive Dose Painting by Number. International Journal of Radiation Oncology*Biology*Physics. 2019;104:207–18.

20. Beddok A, Saint-Martin C, Krhili S, Eddine CA, Champion L, Chilles A, et al. Curative high-dose reirradiation for patients with recurrent head and neck squamous cell carcinoma using IMRT or proton therapy: Outcomes and analysis of patterns of failure. Head Neck. 2022; 10.1002/hed.27153

21. Lau KY, Kan WK, Sze WM, Lee AWM, Chan JKW, Yau TK, et al. Magnetic Resonance for T-staging of nasopharyngeal carcinoma--the most informative pair of sequences. Jpn J Clin Oncol. 2004;34:171–5.

22. Fedorov A, Beichel R, Kalpathy-Cramer J, Finet J, Fillion-Robin J-C, Pujol S, et al. 3D Slicer as an image computing platform for the Quantitative Imaging Network. Magn Reson Imaging. 2012;30:1323–41.

23. Tustison NJ, Gee JC. J.C.: N4ITK: Nicks N3 ITK implementation for MRI bias field correction. Insight Journal. 2009; http://doi.org/10.54294/jculxw.

24. Nioche C, Orlhac F, Boughdad S, Reuzé S, Goya-Outi J, Robert C, et al. LIFEx: A Freeware for Radiomic Feature Calculation in Multimodality Imaging to Accelerate Advances in the Characterization of Tumor Heterogeneity. Cancer Res. 2018;78:4786–9.

25. Dawson LA, Anzai Y, Marsh L, Martel MK, Paulino A, Ship JA, et al. Patterns of local-regional recurrence following parotid-sparing conformal and segmental intensity-modulated radiotherapy for head and neck cancer. Int J Radiat Oncol Biol Phys. 2000;46:1117–26.

26. Robin X, Turck N, Hainard A, Tiberti N, Lisacek F, Sanchez J-C, et al. pROC: an open-source package for R and S+ to analyze and compare ROC curves. BMC Bioinformatics. 2011;12:77.

27. RStudio Team, for R. RStudio, PBC, Boston, MA URL http://www.rstudio.com/. RStudio: Integrated Development Environment for R. [Internet]. RStudio, PBC, Boston, MA; 2021. Available from: http://www.rstudio.com/.

28. Dionisi F, Fiorica F, D'Angelo E, Maddalo M, Giacomelli I, Tornari E, et al. Organs at risk's tolerance and dose limits for head and neck cancer re-irradiation: A literature review. Oral Oncology. 2019;98:35–47.

29. Popovtzer A, Gluck I, Chepeha DB, Teknos TN, Moyer JS, Prince ME, et al. The pattern of failure after reirradiation of recurrent squamous cell head and neck cancer: implications for defining the targets. Int J Radiat Oncol Biol Phys. 2009;74:1342–7.

30. Chen AM, Farwell DG, Luu Q, Cheng S, Donald PJ, Purdy JA. Prospective trial of high-dose reirradiation using daily image guidance with intensity-modulated radiotherapy for recurrent and second primary head-and-neck cancer. Int J Radiat Oncol Biol Phys. 2011;80:669–76.

31. Song J, Yin Y, Wang H, Chang Z, Liu Z, Cui L. A review of original articles published in the emerging field of radiomics. Eur J Radiol. 2020;127:108991.

32. Morin O, Vallières M, Jochems A, Woodruff HC, Valdes G, Braunstein SE, et al. A Deep Look Into the Future of Quantitative Imaging in Oncology: A Statement of Working Principles and Proposal for Change. Int J Radiat Oncol Biol Phys. 2018;102:1074–82.

33. Moskowitz CS, Welch ML, Jacobs MA, Kurland BF, Simpson AL. Radiomic Analysis: Study Design, Statistical Analysis, and Other Bias Mitigation Strategies. Radiology. 2022;211597.

34. Norgeot B, Quer G, Beaulieu-Jones BK, Torkamani A, Dias R, Gianfrancesco M, et al. Minimum information about clinical artificial intelligence modeling: the MI-CLAIM checklist. Nat Med. 2020;26:1320–4.

35. Alfieri S, Romanò R, Bologna M, Calareso G, Corino V, Mirabile A, et al. Prognostic role of pre-treatment magnetic resonance imaging (MRI)-based radiomic analysis in effectively cured head and neck squamous cell carcinoma (HNSCC) patients. Acta Oncol. 2021;60:1192–200.

36. Bogowicz M, Leijenaar RTH, Tanadini-Lang S, Riesterer O, Pruschy M, Studer G, et al. Post-radiochemotherapy PET radiomics in head and neck cancer – The influence of radiomics implementation on the reproducibility of local control tumor models. Radiotherapy and Oncology. 2017;125:385–91.

37. Traylor KS, Koontz N, Mosier K. Squamous Cell Carcinoma: PET/CT and PET/MRI of the Pretreatment and Post-Treatment Neck. Semin Ultrasound CT MR. 2019;40:400–13.

38. Cao C, Xu Y, Huang S, Jiang F, Jin T, Jin Q, et al. Locoregional Extension Patterns of Nasopharyngeal Carcinoma Detected by FDG PET/MR. Front Oncol. 2021;11:763114.

39. Szyszko TA, Cook GJR. PET/CT and PET/MRI in head and neck malignancy. Clin Radiol. 2018;73:60–9.

8. FIGURES CAPTIONS

Figure 1: Examples of failure patterns

This figure illustrates how “in-field” and “outside” recurrences were defined from the PET images (upper part) and the MRI (bottom part). The reirradiated GTV is marked with a black star in the PET and a red star in the MRI. The square represents a physiological hypermetabolism. The recurrent tumor volume (red contour) was identified on PET or MRI at the time of diagnosis of the second recurrence. The green line represents the 95% isodose of the reirradiation plan, for the treatment of the first recurrence GTV segmented on pre-reirradiation PET and/or MRI.

Figure 2: Kaplan-Meier Curve for overall survival (A) and locoregional-free survival (B) of the 55 patients

Figure 3: Flow-chart

Figure 4: Result of the principal component analysis comparing the “recurrence” vs. “no recurrence” groups from MRI features

Figure 5: Result of the principal component analysis comparing the “in-field” vs. “outside” groups from MRI (A) and [18F]-FDG PET features (B)

Table 1: Characteristics of the 55 reirradiated patients

Characteristics	Nb	%
Age (median, IQR)	51 (47.5 – 61)	
Gender		
Male	39	70.9
Female	16	29.1
Retreatment disease site		
Nasopharynx	13	23.6
Nasal cavity and paranasal sinus	11	20
Oropharynx	8	14.5
Nodes (upper jugular group, retropharyngeal, retrostyloid)	7	13
Skull base	5	9
Oral cavity	5	9
Parotid	5	9
Hypopharynx/larynx	1	1.9
Histology		
Squamous cell carcinoma	26	47.3
Undifferentiated carcinoma nasopharyngeal tumor	17	30.9
Adenoid Cystic Carcinoma	10	18.2
Other	2	3.6
Previous treatment course: technique		
3D-CRT	22	40
IMRT	14	25.5
Tomo/VMAT	17	30.9
Proton (PSPT)	2	3.6
Previous treatment course: RT total dose (Gy, [median, IQR])	68 (65.5 – 70)	
Time elapsed since previous irradiation (months, [median, IQR])	35 (20 – 71)	
Surgery before reRT	18	32.7%
reRT Volumes		
GTV (cc, [median, IQR])	22.5 (9.5 – 54.8)	
CTV (cc, [median, IQR])	49.2 (27.3 – 90.4)	
PTV (cc, [median, IQR])	104.4 (58.4 – 172.2)	
reRT techniques		
3D-CRT	1	1.9
IMRT	15	27.3
Tomo/VMAT	12	21.8
Proton (PSPT)	27	49
Overall treatment time during reRT (days, [median, IQR])	55 (48.8 – 58.3)	
Dose in target volumes		
$D_{95\%}$ CTV (Gy RBE, [median, IQR])	57.2 (50.7 – 61.5)	
$D_{95\%}$ PTV (Gy RBE, [median, IQR])	61.5 (56.5 – 65.3)	
Locoregional recurrences	40	72
In-field	18	45
Outside	22	55
Nodes	2	9
Mucosa	20	81
Imaging before reirradiation	48	87.2
[18F]-FDG PET	30	54.5
Contrast Enhancement Fat Sat CUBE T1 MRI	33	60

Figure 1:

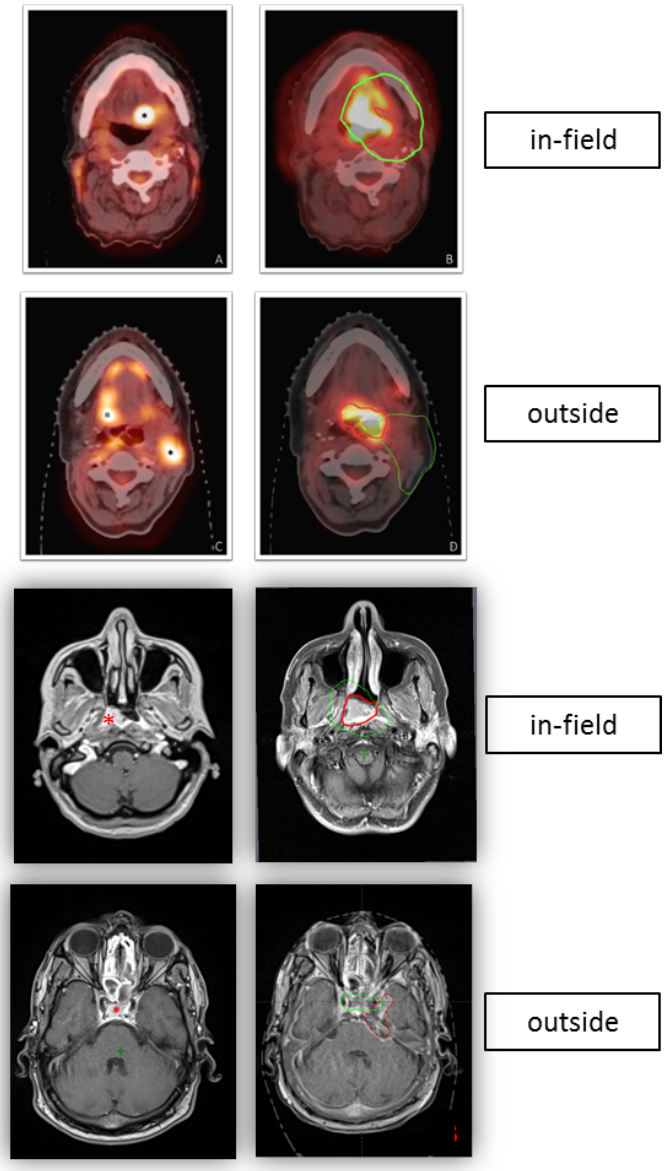

Figure 2:

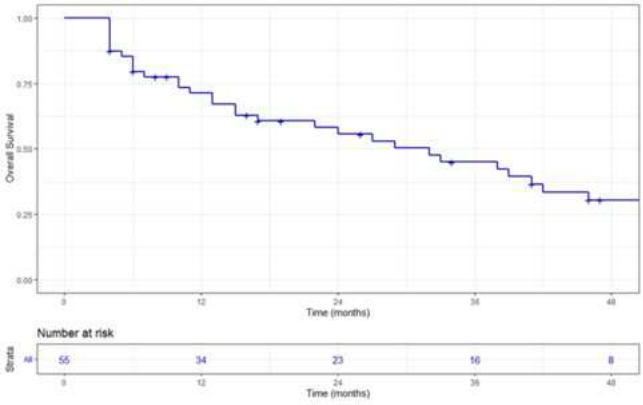
Overall Survival
1.00
0.75
0.50
0.25
0.00
0
12
24
36
48
Time (months)
Number at risk
Strata
All
55
34
23
16
8
Time (months)

A

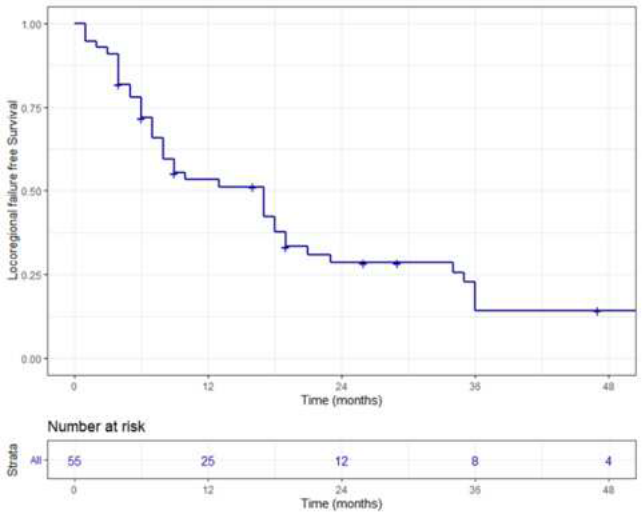
Locoregional failure free Survival
1.00
0.75
0.50
0.25
0.00
0
12
24
36
48
Time (months)
Number at risk
Strata
All
55
25
12
8
4
Time (months)

B

Figure 3:

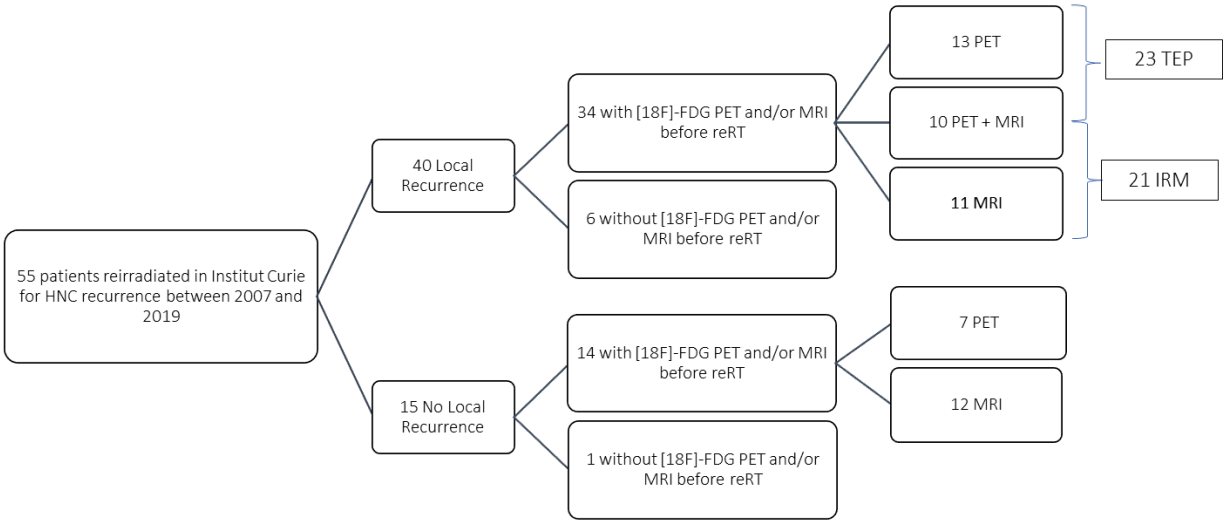
55 patients reirradiated in Institut Curie for HNC recurrence between 2007 and 2019
40 Local Recurrence
15 No Local Recurrence
34 with [18F]-FDG PET and/or MRI before reRT
6 without [18F]-FDG PET and/or MRI before reRT
14 with [18F]-FDG PET and/or MRI before reRT
1 without [18F]-FDG PET and/or MRI before reRT
13 PET
10 PET + MRI
11 MRI
7 PET
12 MRI
23 TEP
21 IRM

Figure 4:

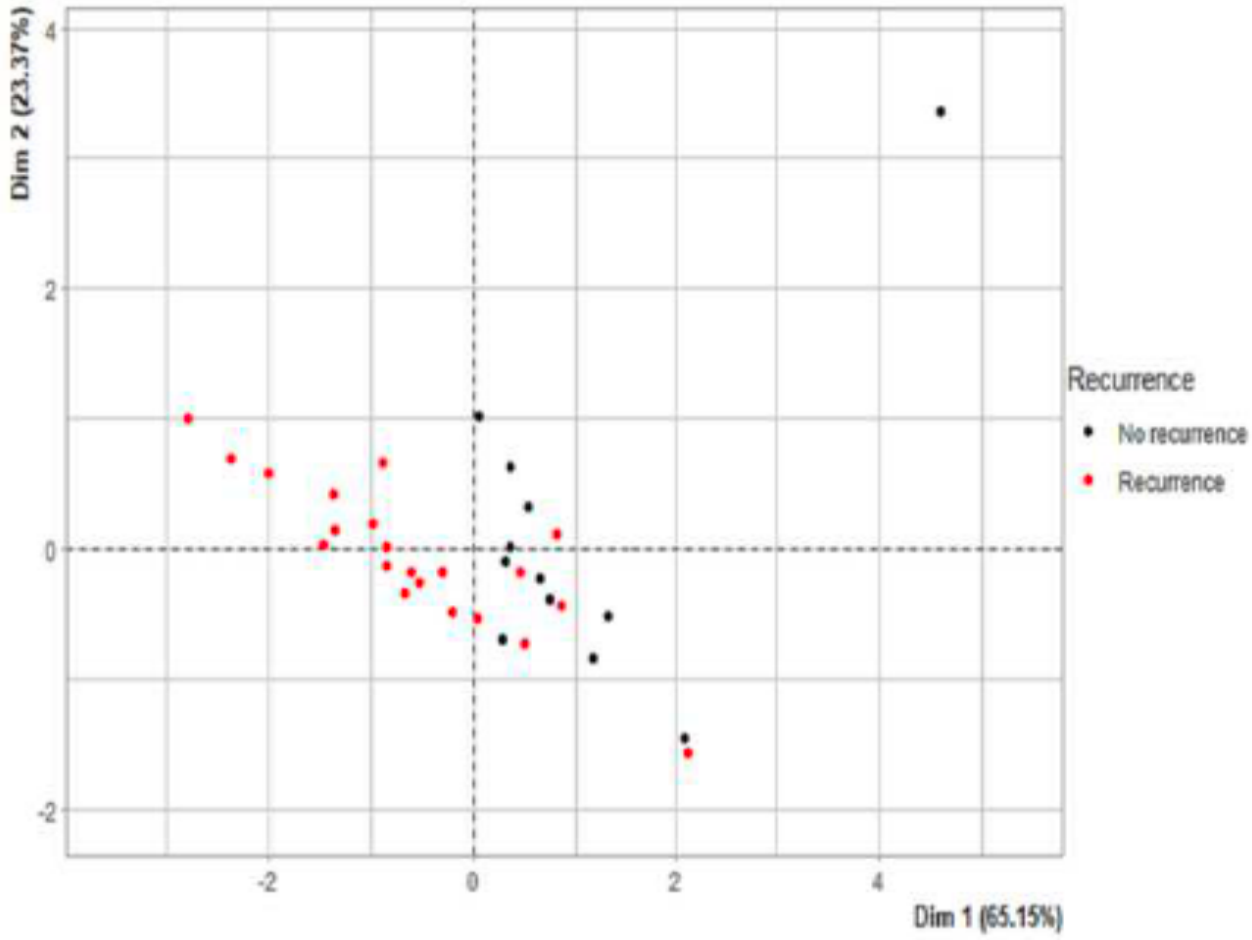
Dim 2 (23.37%)
4
2
0
-2
-2
0
2
4
Dim 1 (65.15%)
Recurrence
No recurrence
Recurrence

Figure 5:

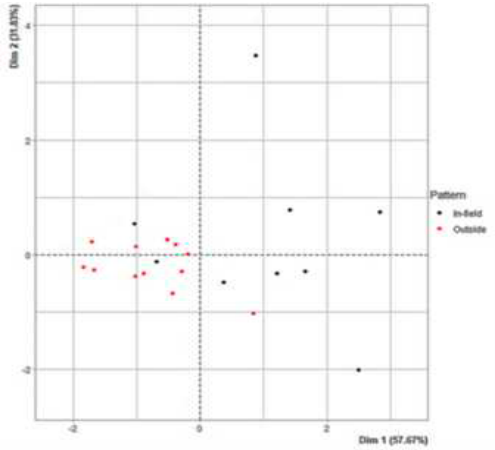
Dim 2 (31.83%)
Dim 1 (57.67%)
Pattern
In-field
Outside

A

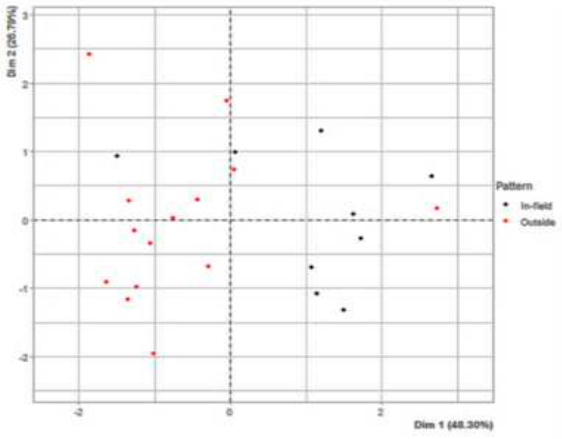
Dim 2 (26.79%)
Dim 1 (48.30%)
Pattern
In-field
Outside

B